

High-Accuracy Calibration of the HXDS Flow Proportional Counter for AXAF at the PTB Laboratory at BESSY

J.M. Auerhammer, G. Brandt, F. Scholze, R. Thornagel, and G. Ulm
Physikalisch-Technische Bundesanstalt, Abbestr. 2-12, 10587 Berlin, Germany

B.J. Wargelin, W.C. Mc Dermott, T.J. Norton, I.N. Evans, and E.M. Kellogg
Smithsonian Astrophysical Observatory, 60 Garden Street, Cambridge, MA 02138, U.S.A.

ABSTRACT

The Smithsonian Astrophysical Observatory uses the HRMA X-ray Detection System (HXDS) to calibrate the High-Resolution Mirror Assembly (HRMA) of the Advanced X-ray Astrophysics Facility AXAF. Apart from two high-purity-germanium solid-state detectors (SSDs) with good energy resolution and very high efficiency at higher energies, the detection system comprises seven flow proportional counters (FPCs) and one microchannel-plate High-Speed Imager. For the lower energy range, the FPCs are more appropriate. They have been calibrated at the radiometry laboratory of the Physikalisch-Technische Bundesanstalt, using the electron storage ring BESSY. For the determination of the absolute quantum efficiency two methods have been applied.

First, the detector response was measured in the lower energy range 0.1 keV to 1.7 keV at several discrete energies using monochromatized radiation. The absolute photon flux has been determined by Si n-on-p photodiodes, calibrated against a cryogenic electrical-substitution radiometer used as primary detector standard. The second method uses the undispersed synchrotron radiation emitted by a bending magnet of the primary source standard BESSY, which can be calculated very accurately. Combining both measurements the determination of the detection efficiency over the entire desired spectral range (0.1 keV to 10 keV) was possible with a typical relative uncertainty around 1% to 2% in the central energy range (0.2 keV to 1.7 keV).

Keywords: proportional counters, detectors, calibration, x-rays, synchrotron radiation, primary detector standard

1. INTRODUCTION

The calibration of the High-Resolution Mirror Assembly (HRMA) for the Advanced X-ray Astrophysics Facility AXAF was performed by the Smithsonian Astrophysical Observatory (SAO). It is expected that AXAF yields data from objects emitting in the x-ray region, improving the knowledge about neutron stars, black holes, debris from exploding stars, quasars, and hot gas in galaxies. A prerequisite for the extraction of the precise number of x-ray events from a spectrum is the knowledge of the x-ray response of the AXAF-system to about 1% to 2%.

In order to achieve this goal, not only the detectors used for high-resolution energy-dispersive spectroscopy have to be calibrated with this accuracy, but also the optics used for high resolution imaging. For this, ground-based x-ray detectors are used as detector standards. For the higher energy range high-purity germanium (HPGe) detectors¹ are used and for the lower energy range flow-proportional counters (FPCs)². In order to serve as secondary standards the detectors have to undergo high-accuracy calibrations themselves. These calibrations and the determination of the response functions have been carried out for two FPCs in the laboratory of the Physikalisch-

Technische Bundesanstalt (PTB) at BESSY and are subject of this paper. The calibration of the HPGe-detectors has been performed earlier³.

Unlike x-ray radiation standards provided by radioactive sources, the synchrotron radiation at BESSY provides a continuous spectrum and the spectral flux can be calculated from first principles. For the calibration of the FPCs, undispersed and monochromatized synchrotron radiation (SR) were used, where BESSY and an electrical substitution radiometer serve as primary standards, respectively. Both methods have been established at the PTB radiometry laboratory⁴⁻⁶. The combination of these methods provides an ideal tool for high-accuracy detector calibration.

2. DETECTOR DESCRIPTION

2.1. Flow Proportional Counter

In order to be able to cover a large energy range, flow proportional counters (FPCs) were chosen having a thin window for a good low-energy quantum efficiency (QE), a deep gas volume for good high-energy QE, and a large window area for good counting statistics². The window consists of thin polyimide (1 μm) with a 20 nm Al-coating on the inside surface and serves as a barrier between the gas and the vacuum system. The detector volume is continuously supplied with a gas mixture of 90% argon and 10% methane. The argon provides most of the opacity, while the methane acts as quench gas. The gas pressure is kept around 520 mbar. For the calibration measurements the count rate was kept below 5000 counts/s in order to keep pileup events and deadtime low.

If the detector is irradiated with a known spectral flux $\phi(E)$, the measured spectrum or pulse height distribution $C(E)$ is given by

$$C(E) = \int_0^{\infty} R(E', E) \varepsilon(E') \phi(E') dE' \quad (1)$$

The detection efficiency $\varepsilon(E)$ can be determined with high accuracy by measuring the detector response using monochromatized radiation of high purity, by modeling the response function $R(E', E)$ over the desired photon energy range on the basis of the physical properties of the photon detection process and by calculating the absolute photon flux $\phi(E)$ from first principles, i.e. using BESSY as primary source standard, or by measuring $\phi(E)$ of monochromatized radiation using a detector standard, respectively.

The determination of the efficiency for the FPC is based on the assumption that photons produce a pulse when they are absorbed in the fill gas argon, after they are transmitted through the window (transmittance τ_C , τ_N , τ_O and τ_{Al}). However, Auger- and photoelectrons produced in the window might generate a pulse with the probability P_{window} once they get into the fill gas. The detection efficiency can be expressed as

$$\varepsilon(E) = (1 - \tau_{Ar}) \tau_C \tau_N \tau_O \tau_{Al} + P_{\text{window}} \quad (2)$$

2.2. Detector Response Functions

The response functions are determined from measurements of the pulse height distribution produced in the FPC at discrete energies E_0 , i.e. $\phi(E) = \phi_0 \delta(E - E_0)$. From the knowledge of the response functions at several energies, the determination of the response function matrix is possible.

Monochromatized radiation of high spectral purity was provided by the SX-700 beamline of the PTB radiometry laboratory at BESSY⁷ and by the double crystal monochromator of BESSY⁸. Typical measured spectra taken at four different incident x-ray energies and best-fit model functions superimposed, are shown in Fig. 1. A spectrum consists of a broadened main peak reflecting the finite energy resolution, pileup events and a low energy shelf due to Auger- and photoelectrons from the detector window and fill gas.

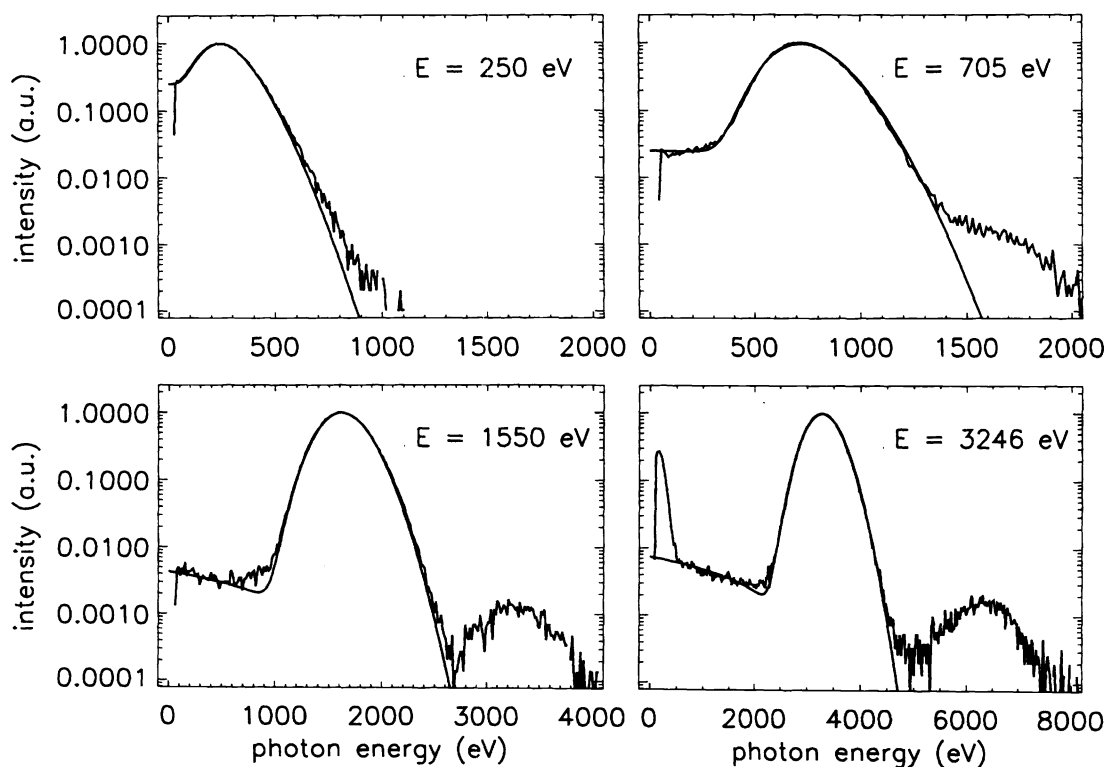


Fig. 1: Measured and modeled response functions of the FPC detector at photon energies of 250 eV, 705 eV, 1550 eV and 3246 eV.

At $E = 3246$ eV and 1550 eV the pileup peak is clearly separated from the photo peak. Due to the escape of Ar-K fluorescence photons a peak is appearing on the left side of the spectrum at 3246 eV. At 705 eV the pileup peak overlaps with the main peak, while at 250 eV it has merged into the main peak. Pileup is assumed to be independent of photon energy, but dependent on count rate. From measurements at different count rates r_c using an electronic pulser, a relative pileup contribution of $N_p = t_p r_c$, with $t_p = 0.77$ μ s has been found. Having $r_c = 5000$ counts/s, the relative pileup contribution is 0.39%.

The measured pulse-height distribution of the main peak can be best modeled by a Prescott function⁹ which has been applied to the spectrum produced by proportional counters before¹⁰. The Prescott function can reproduce the skewness of the peak having the following form:

$$P(E) = \frac{P_0 m^{1/4}}{\sqrt{4\pi} Q E^{3/4}} \exp\left[-\frac{(\sqrt{m}-\sqrt{E})^2}{Q}\right] \quad (3)$$

where P is the number of counts per energy interval, P_0 the area of the Prescott function, m the mean energy of the main peak and Q the width parameter of the Prescott function. To fully describe the measured response function, a low energy distribution - a shelf - described by

$$S(E) = (a + bE)\text{erf}(mE) \quad (4)$$

has to be added, where a and b denote the offset and slope of the shelf. The detector response function R can now be expressed as $R(E) = P(E) + S(E)$. In this model, the escape peak is not yet included.

The energy dependence of the content in the shelf relative to the total spectrum is displayed in Fig. 2. At lower energies the contribution of the shelf gets quite substantial (up to 25%), while it decreases to about 1% at higher energies. At absorption edges always a sharp rise is seen. Measured values are shown as open circles. The solid line in Fig. 2 shows a calculation of the shelf based on the model developed for energy-dispersive Si(Li) detectors¹¹. Here, the contributions to the shelf are the escape-probability of photo- or Auger-electrons arising from photons absorbed in the Ar counting gas (dashed line in Fig. 2) and the probability that photo- or Auger-electrons arising from photons absorbed in the window (mainly C and Al) penetrate into the counting gas. For photon energies below the Ar K edge (3206 eV) the contribution from the window clearly dominates the total shelf contribution.

The Prescott width Q stays almost constant around 14 eV in the investigated energy range. It is related to the variance σ_p^2 of the Prescott distribution by $\sigma_p^2 = 2 m Q$. A nearly constant width Q confirms the $E_0^{1/2}$ dependence of σ_p .

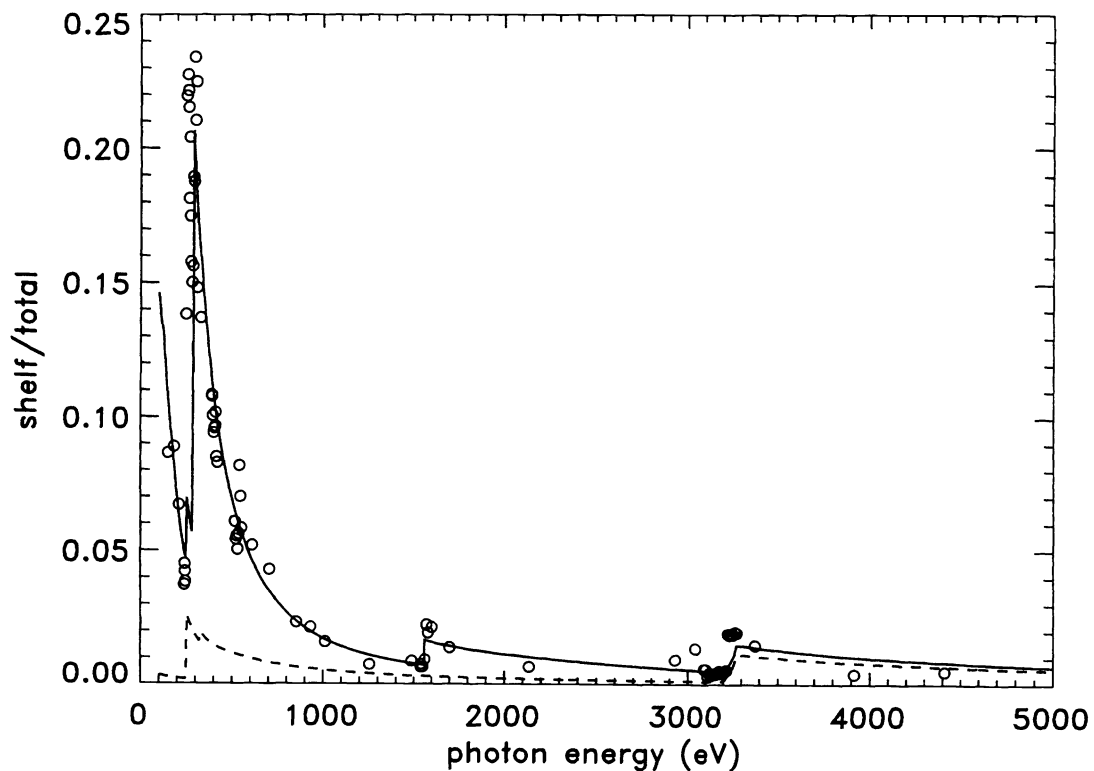


Fig. 2: Energy dependence of the shelf relative to the total spectrum (peak plus shelf). The solid line represents a calculation for the total shelf and the dashed line is the calculated contribution from argon only.

3. CALIBRATION WITH MONOCHROMATIZED SYNCHROTRON RADIATION

The calibration was conducted at the plane grating monochromator SX-700 radiometry beamline. The experimental setup and the methods for performing the detector calibration using monochromatized SR are described in this chapter. The details of this already well established method can be found elsewhere³.

For high-accuracy detector calibration with monochromatized SR, well characterized radiation is required. The SX-700 radiometry beamline is specially designed to provide radiation of high spectral purity in the range 40 eV to 1500 eV. It is described in detail in Ref. 7. The contents of harmonic diffraction orders can be kept below 0.15% with appropriate filters for energies between 250 eV to 1500 eV. The stray light becomes significant at 1.5 keV, where it rises from 3% up to 10% at 1.7 keV.

To obtain the quantum efficiency of the FPC detector, the response of the FPC was compared to the response of a detector standard. The absolute flux determination is done by using Si n-on-p photodiodes as transfer detector standards, which are calibrated against a cryogenic electrical-substitution radiometer used as a primary standard¹². The spectral responsivity of the photodiodes has been determined with a relative uncertainty of less than 0.5% in the photon energy range below 1500 eV. In order to determine the total number of counts of the FPC a precise knowledge of the detector response function is required for photon energies below 700 eV. As already mentioned the count rate on the FPC detector had to be limited to 5000 counts/s, while the photodiodes are operated with a flux in the order of 10^7 photons/s. Thus, the flux has to be reduced by several orders of magnitude. It has been shown that the photon flux behind the monochromator scales linearly with the stored electron current³. Reducing the stored electron current is thus an elegant method to lower and adjust the photon flux in the measured energy range with an uncertainty of better than one percent.

To extract the total number of photons, the measured FPC response functions were analyzed at discrete energies. A fitting procedure was applied taking pileup effects into account (see 2.2). The absolute flux has been measured with the photodiodes for discrete photon energies within the energy range of the monochromator, i.e. between 100 eV and 1700 eV with a relative uncertainty of 1% to 2%. A comparison with the count rate obtained at the FPC at these energies yields the quantum efficiency (Fig. 3, open squares). The carbon edge at 284 eV is very pronounced reducing the quantum efficiency to less than 1%, but also edges due to x-ray absorption in nitrogen (392 eV), oxygen (532 eV) and aluminum (1.48 keV) are visible. At low energies ($E < 1500$ eV) the quantum efficiency is essentially determined by the window transmission, since the detector filling gas is opaque in this region. To corroborate this, the transmission of a detached aluminum coated polyimide window was measured. The result is plotted in Fig. 3 as a dashed line. It agrees with the absolute QE within 5% in the range $E > 600$ eV. Around the edges the transmission becomes very sensitive to the degree of stretching of the window.

The measurements can be compared with Eq. 2. A best fit to the derived quantum efficiency yields for the effective thicknesses for carbon 500 nm, for nitrogen 100 nm, for oxygen 300 nm and for aluminum 20 nm. Hereby, the calculated shelf contribution P_{window} is also considered. In the range 300 eV to 1500 eV the absorption of argon is close to unity, so that the effective thickness of argon cannot be determined accurately. Above 1500 eV, however, these measurements indicate an incomplete absorption of the incident photons in the FPC.

The uncertainties in this measurement depend on many parameters. The sources of the uncertainty are related to the total flux determination, to the purity of the monochromatized SR, to the detector and to the data analysis. The total uncertainty stays below 1% in the range 400 eV to 1200 eV, below 2% in the range 1200 eV to 1700 eV and 200 eV to 400 eV except around the C K edge (265 eV to 330 eV), where the harmonic order content of the radiation and the dark current of the photodiode rise the uncertainty to values up to 5%. All other contributions stay around 0.1% to 1%. At low photon energies ($E < 250$ eV) there is the general problem that due to the very low quantum efficiency for the first diffraction order, the influence of higher harmonics and electronic discrimination problems due to the detector noise gets stronger, increasing the uncertainty. Furthermore, at low photon energies the harmonic orders and pileup events are energetically too close to the main peak in order to get resolved. Above 1500 eV the main source of uncertainty is the increasing stray light contribution.

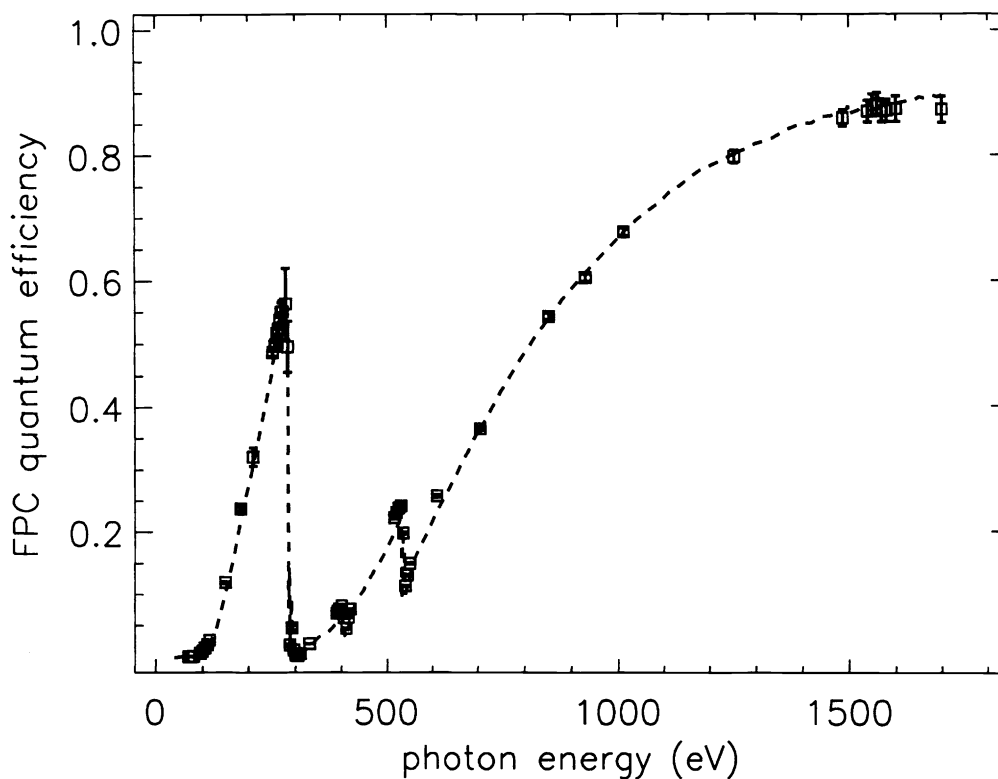


Fig. 3: Absolute quantum efficiency versus photon energy determined from the ratio of total counts of the measured response to the number of incident photons (open squares). In comparison the transmittance of the polyimide window (dashed line) is shown.

4. CALIBRATION WITH UNDISPERSED SYNCHROTRON RADIATION

4.1. Calculation of the Absolute Photon Flux

The spectral photon flux $\phi(E)$ emitted from electrons passing a bending magnet of the electron storage ring BESSY can be calculated by fundamental laws of electrodynamics. Behind an angle-limiting aperture with radius r in front of the detector at a distance d from the source point, the flux is a function of seven parameters: the electron energy W , the magnetic induction of the bending magnet B , the electron beam current I_R , the effective divergence of the electron beam Σ_y , the view angle ψ relative to the electron orbit plane, the aperture radius r and the distance d . All these parameters were determined individually for each measurement with an overall uncertainty of below 2%. The methods of determining these parameters precisely are described elsewhere³. Table 1 lists the values and uncertainties of the measured electron storage ring and geometric parameters.

parameter	symbol	value
Electron energy	W	798.080(15) MeV
Magnetic induction	B	1.490738(12) T
Effective divergence	Σ_y	$(10^{+5}_{-10}) \mu\text{rad}$
Distance source-aperture	d	17000(3) mm
Aperture radius	r	0.750(8) mm
Emission angle	ψ	0(9) μrad
Electron beam current	I_R	several electrons

Table 1: Typical uncertainties of the electron storage ring and geometry parameters.

4.2. Measured and Calculated Pulse Height Distribution

The pulse height spectrum $C(E)$ measured on the FPC can be reproduced by convoluting the spectral distribution incident on the detector $\phi(E)$ and the detector response function $R(E',E)$ multiplied by the detector efficiency $\varepsilon(E)$ (see Eq. 1 and 2). The flux $\phi(E)$ is calculated from first principles using the parameters listed in Tab. 1. The response matrix is determined from measurements of the response function at discrete energies in the range 100 eV to 5900 eV. The window transmittance has been derived from the measurements with low energy monochromatized radiation. Taking those parameters as known, the transmittance of the counting gas at higher photon energies could be determined from $C(E)$. The contribution from Auger- and photoelectrons generating a pulse is taken from the analysis of the response functions (see Eq. 4 and 2.2). The determination of the Ar thickness and thus its uncertainty is affected by the combined effects of pileup, possible shifts of the energy scale and incorrect absorption data. Differences between the calculated and the measured spectrum $C(E)$ may be also due to inaccuracies of the detector model, in particular at the absorption edges.

A comparison of measured and calculated pulse-height distribution for 108 electrons corresponding to a beam current of 83.1276 pA (1 electron corresponds to 0.7697 pA) is displayed in Fig. 4 (upper spectrum). The dashed line shows the calculation. In order to determine the effective thickness of the argon counting gas an additional measurement with an Fe filter placed in front of the detector suppressing the lower energy photons ($E < 1000$ eV) was carried out (see lower spectrum in Fig. 4). Both spectra were normalized to one electron. The argon edge becomes visible making a determination of the effective thickness possible. Furthermore, a relative pileup contribution of 0.36% is assumed according to a count rate of 4640 c/s. The spectrum measured without filter agrees within the statistical uncertainty up to photon energies of 3000 eV except at the vicinity of the carbon K edge. For the measurement with the Fe filter the count rate below the Fe L edge exceeds significantly the calculated values due to fluorescence from the filter.

The quantum efficiency in the range 0.1 eV to 10 keV can be calculated by Eq. 2, using the derived best-fit parameters for the window thickness and the counting gas absorption. The result is displayed in Fig. 5 as a solid line. Superimposed are the discrete values measured with monochromatized SR (crosses). Below and above the Ar K edge ($E > 6$ keV) the efficiency depends critically on the absorption in argon.

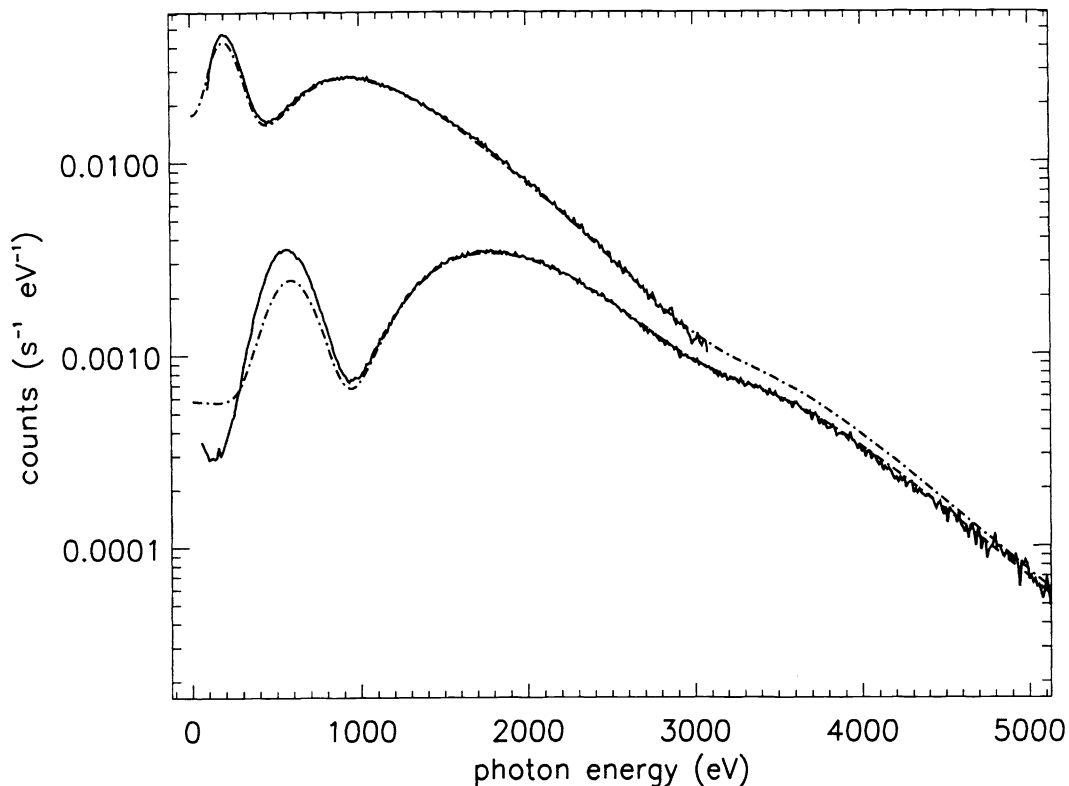


Fig. 4: The measured pulse height spectrum of the FPC taken without a filter (upper spectrum) and normalized to one electron agrees quite well with the calculated undispersed spectrum (dash-dotted line). The lower spectrum is taken with a Fe-filter showing the Ar-K edge. The calculation according to Eq. 1 is shown as a dash-dotted line.

Note, that in the measured spectrum without filter only the strong absorption of carbon can be identified. All other structures of the transmittance of window and coating are smeared out due to the moderate energy resolution of the detector. Any finestructure modifying $\epsilon(E)$ by as much as 20% cannot be detected. The detector calibration with monochromatized SR in this energy range was therefore essential.

5. DISCUSSION

The detection efficiency of a flow proportional counter was measured by using two independent methods using monochromatized and undispersed SR. Both methods for the determination of the quantum efficiency require the knowledge of the detector response function which was measured and could be modeled very well with Prescott functions and a flat shelf. The shelf according to Eq. 4 is a good estimation for photon energies above 250 eV. Below 250 eV shelf and main peak cannot be distinguished clearly anymore. The uncertainty of the shelf is estimated to be about 5% above 250 eV and below about 20%. The shelf contribution can be approximated very well

by calculating the probability of the escape of Auger- and photoelectrons from the count gas and that Auger- and photoelectrons generated in the window produce a pulse.

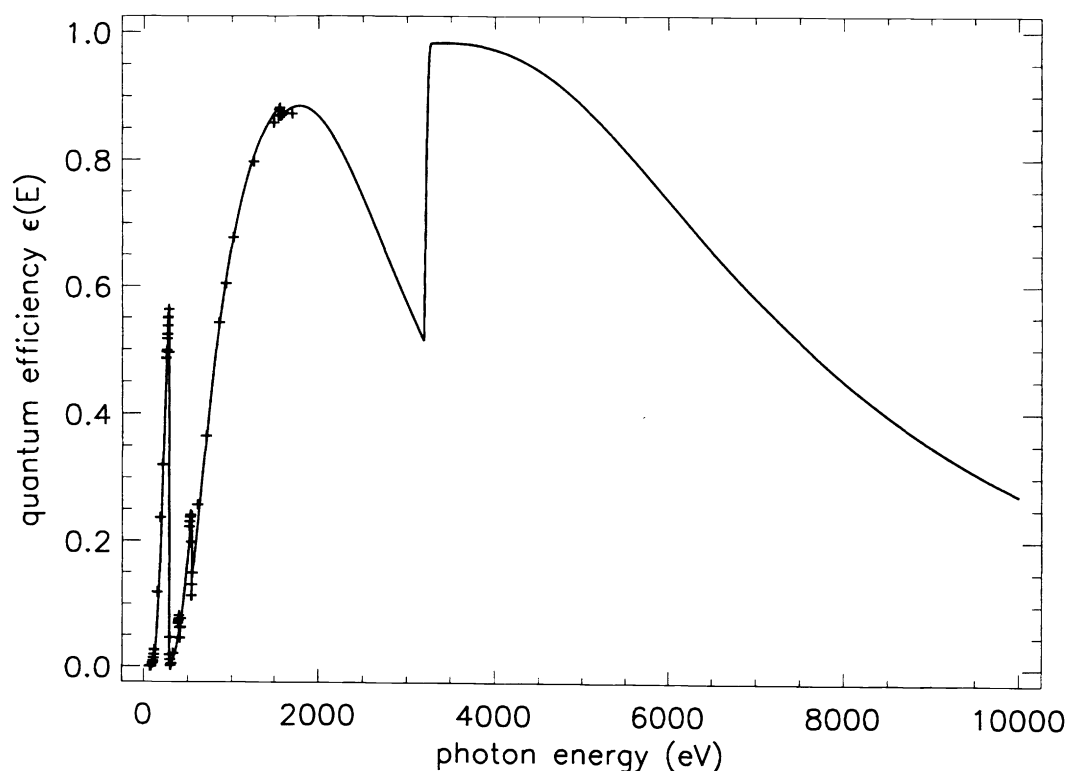


Fig. 5: Preliminary results of the quantum efficiency derived from the measurement of undispersed SR (solid line) in the range 0.1 keV to 7 keV. As a comparison $\epsilon(E)$ derived from the measurement with monochromatized SR is shown as crosses.

The determination of the efficiency $\epsilon(E)$ with monochromatized SR is more accurate in the lower photon energy range 100 eV to 1700 eV compared to the measurements with undispersed radiation. The influence of weak absorption at the N and O edge (small effective thickness) is seen as well as the finestructures around the Al edge (1560 eV to 1700 eV). At low photon energies, when $\epsilon(E)$ is very low (<10%) the absence of high energy photons, creating background counts in the low energy region, has the advantage, that $\epsilon(E)$ could be measured with a low relative uncertainty facilitating an accurate determination of the effective thicknesses of the elements in the window.

The measurement with undispersed SR has the advantage of extending the photon energy range up to possibly 10 keV. Due to the very low efficiency at photon energies below 200 eV the count rate in the undispersed spectrum is dominated from photons of higher energy. The data obtained for energies below 200 eV are not reliable with this method. Also the Al-XAFS structure and the N and O edges were not visible in the undispersed spectrum.

The calibration method using monochromatized SR ensures the determination of the efficiency with an accuracy of 1% to 2% in the photon energy range from 200 eV and 1700 eV. However, below 200 eV where the photo-peak starts to overlap with the noise such an accuracy is not guaranteed.

CONCLUSION

The absolute quantum efficiency $\epsilon(E)$ of the HXDS flow proportional counters have been determined on the basis of two different primary radiometric standards. The determination of $\epsilon(E)$ using monochromatized radiation and Si photodiodes as transfer detector standards was performed in the photon energy range 100 eV and 1700 eV. Using undispersed calculable synchrotron radiation emitted by a bending magnet of the primary source standard BESSY extended the calibration range to about 6 keV. Both methods have been already used to completely characterize the HPGe detectors for AXAF calibration and could now be successfully applied to the Flow Proportional Counters. The combination of both methods yields low uncertainties in the entire range.

Both methods require measuring and modeling of the response functions in the photon energy range 0.1 eV to 6 keV. A model function consisting of a Prescott distribution and a flat shelf described the measured detector response functions quite well. The low energy shelf contributes 1% to 25% to the total response. The measured response to undispersed SR agrees with the calculation within the statistical uncertainty between 200 eV and 4000 eV except in the vicinity of the C K edge. Using monochromatized SR and Si n-on-p photodiodes as transfer detector standards, it was possible to pay particular attention to the low energy range where the FPCs are still sensitive, to the weaker absorption edges (N,O) and to the finestructures at the Al absorption edge.

The calibration using monochromatized SR is up to now limited to the energy range below 1700 eV due to the increasing stray light at the SX-700 beamline. At the electron storage ring BESSY II which will be available for users by the end of the year '98, the spectral range will be extended up to 10 keV for monochromatized SR at the PTB's four crystal monochromator¹³. Calculable undispersed SR will be available for photon energies up to 60 keV.

REFERENCES

1. W.C. McDermott, E.M. Kellogg, B.J. Wargelin, I.N. Evans, S.A. Vitek, E.Y. Tsiang, D.J.A. Schwartz, R. Edgar, S. Kraft, F. Scholze, R. Thornagel, G. Ulm, M. Weisskopf, S. Odell, A. Tennant, J. Koldziejczak, and G. Zirnstein, "The AXAF HXDS germanium solid state detectors", *Proc. SPIE* **3113**, pp. 535-543, 1997.
2. B.J. Wargelin, E.M. Kellogg, W.C. McDermott, I.N. Evans, and S.A. Vitek, "AXAF Calibration: The HXDS Flow Proportional Counters", *Proc. SPIE* **3113**, pp. 526-534, 1997.
3. S. Kraft, F. Scholze, R. Thornagel, G. Ulm, W.C. McDermott, E.M. Kellogg, "High Accuracy Calibration of the HXDS HPGe Detector at the PTB Radiometric Laboratory at BESSY", *Proc. SPIE* **3114**, pp. 101-112, 1997.
4. H. Rabus, F. Scholze, R. Thornagel, G. Ulm, "Detector calibration at the PTB radiometry laboratory at BESSY", *Nucl. Instr. Meth.* **A377**, pp. 209-216, 1996.
5. R. Thornagel, J. Fischer, R. Friedrich, and M. Stock, G. Ulm and B. Wende, "The electron storage ring BESSY as a primary standard source - a radiometric comparison with a cryogenic electrical substitution radiometer in the visible", *Metrologia* **32**, pp. 459-462, 1995.
6. D. Arnold and G. Ulm, "Electron storage ring BESSY at a source of calculable spectral photon flux in the x-ray region", *Rev. Sci. Instrum.* **63**, pp. 1539-1542, 1992.
7. F. Scholze, M. Krumrey, P. Müller, and D. Fuchs, "Plane grating radiometry beamline for VUV-radiometry", *Rev. Sci. Instrum.* **65**, pp. 3229-3232, 1994.
8. J. Feldhaus, F. Schäfers and W. Peatman, "The Crystal Monochromator at BESSY", *Proc. SPIE* **733**, pp. 242-246, 1984.

9. J. Prescott, "Photomultiplier single-electron statistics and the shape of the ideal scintillation line", *Nucl. Instr. Meth.* **22**, pp. 256-268, 1963.
10. C. Budtz-Jorgensen, C. Olesen, H.W. Schnopper, T. Lederer, F. Scholze, and G. Ulm, "The response functions of the HEPC/LEPC detector system measured in the Xe L edge region", *Nucl. Instr. Meth. A* **367**, 83-87, 1995.
11. F. Scholze, G. Ulm, "Characterization of a windowless Si(Li) detector in the photon energy range 0.1 to 5 keV", *Nucl. Instr. Meth.* **A339**, pp. 49-54, 1994.
12. H. Rabus, V. Persch, and G. Ulm, "Synchrotron-radiation operated cryogenic electrical-substitution radiometer as the high-accuracy primary detector standard in the ultraviolet, vacuum-ultraviolet, and soft-x-ray spectral ranges", *Applied Optics* **107**, pp. 5421-5440, 1997.
13. G. Ulm, B. Beckhoff, R. Klein, M.K. Krumrey, H. Rabus, R. Thornagel, "The PTB radiometry laboratory at the BESSY II electron storage ring", *these proceedings*